Supplementary Online Information:

Atmospheric oxygenation driven by unsteady growth of the continental sedimentary reservoir

Earth and Planetary Science Letters 460:68-75

Jon M. Husson & Shanan E. Peters

S1 The global nature of the North American sedimentary record

In addition to comparing Macrostrat (Fig. S1) to global sediment volume surveys (see Methods and Fig. 3), another approach to testing the global nature of the continental sedimentation trends portrayed in Fig. 1 of the main text is comparison to data from geological maps (Fig. S2). The Macrostrat database currently contains 1,888,733 geologic map polygons. Map coverage at relatively coarse spatial scales is globally complete, consisting of 7,705 polygons (GSC, 1995). Finer spatial resolution is available at certain regions of the globe. For example, in addition to coverage by the global map, North America is covered also by 39,397 polygons from the Geological Map of North America ('GMNA', Garrity and Soller, 2009). These maps - the globe at a small scale and GMNA at a larger scale - are shown in Fig. S2a, and were used in the analyses presented in Fig. S2b.

In addition to age estimates, most surface bedrock polygons have text descriptions related to lithology and other rock properties. Temporal and lithological resolution vary from map to map, with the global scale map being the most generalized. However, every polygon used in this analysis is resolvable at least to the ∼period level in the Phanerozoic, and ∼era level in the Precambrian, and can be classified as either sedimentary, volcanic, plutonic or metamorphic, allowing for the sediment area time series in Fig. S2b. to be constructed. The map time series are compared to Macrostrat's model of sedimentary areal coverage with time. These comparisons are necessarily qualitative, owing to the coarse temporal and lithological resolution of map data and the fact that maps cannot account for sedimentary rocks that are buried by younger sediments (unlike Macrostrat, which attempts to capture sub-surface sediment expression and areal extent; Fig. S1).

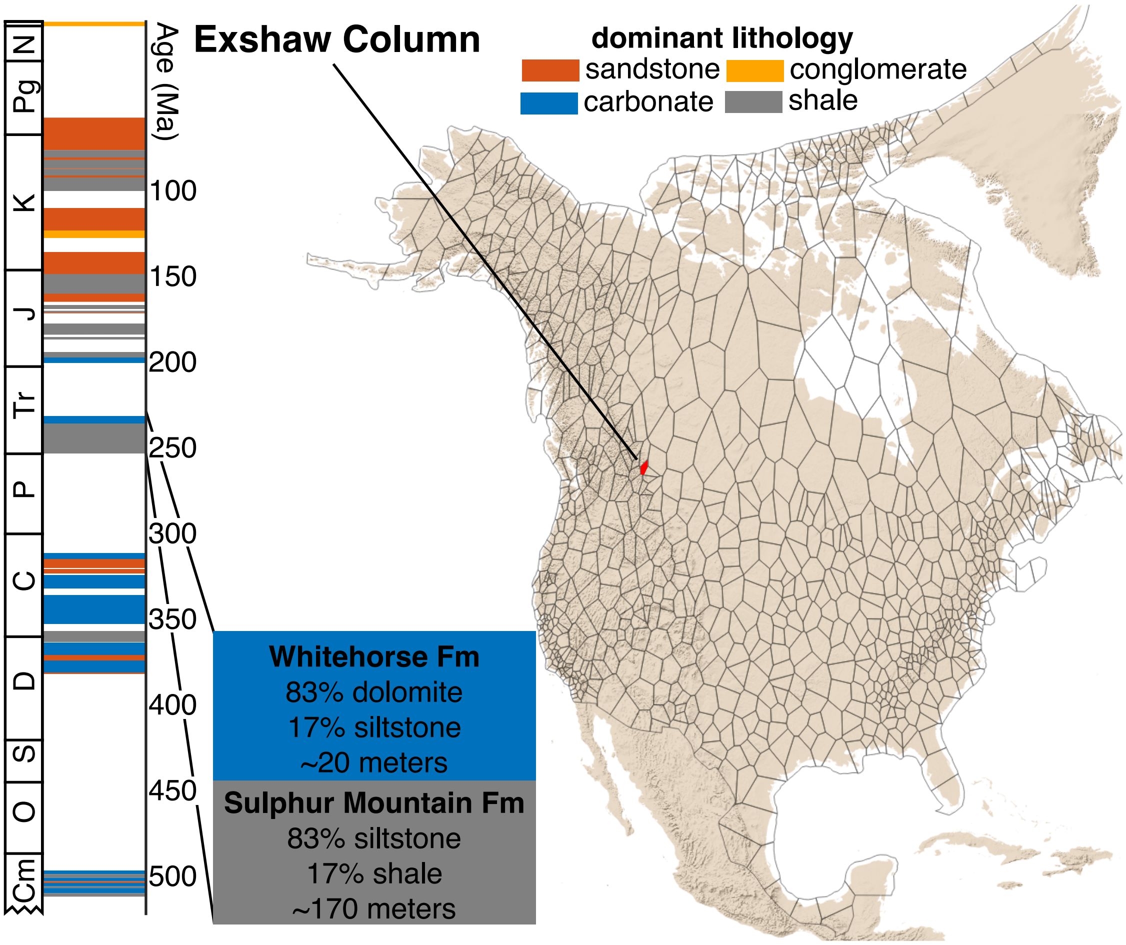

Figure S1: **North American Macrostrat.** This map outlines the areal extent of Macrostrat's 949 columns that are used to describe the lithostratigraphy of North America, as well as example data from the 'Exshaw' column of western Canada, with units displayed chronostratigraphically.

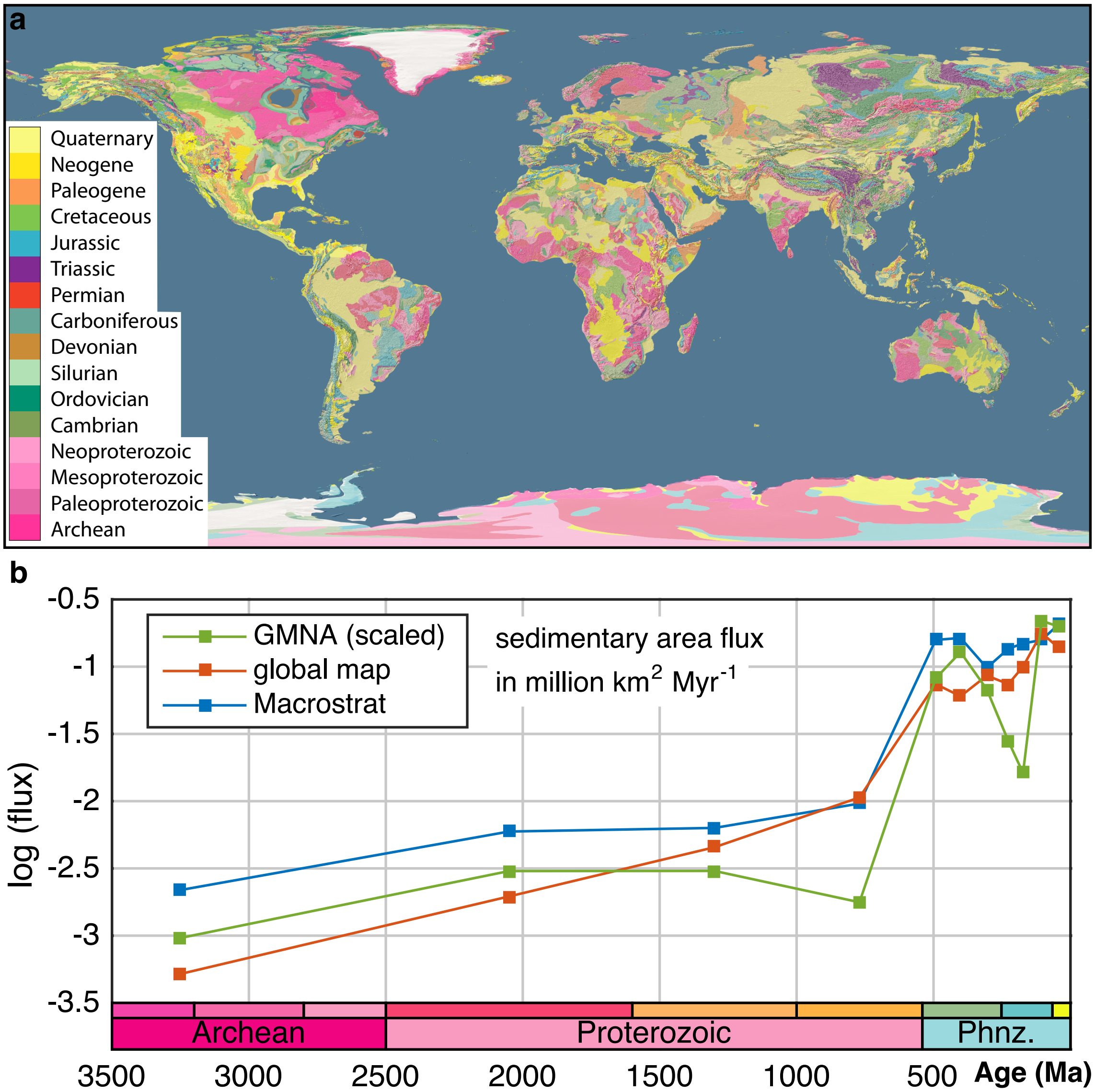

Figure S2: **Geological map data.** **(a)** Global (GSC, 1995) and North American (Garrity and Soller, 2009) geologic map data, color-coded by age. **(b)** The sedimentary data shown in **(a)** is displayed as a time-series of sediment area, normalized by bin duration (red and green curves), along with the sediment area model from Macrostrat (blue curve).

However, according to Fig. S2a, North America contains 15.9% of total exposed Precambrian sedimentary rock (10,155,575 km^2) – nearly identical to North America's geographic footprint relative to total continental crust (14.6%) on this global map. This concordance suggests that North America's Precambrian record contains 1% more Precambrian rock than is expected from its areal extent, if North America represents a roughly random temporal sampling of the continental sedimentary rock record. While this summary value may not hold true at all temporal scales within the Precambrian – for example, North American exposure of the Tonian sediments compared to the global value – it does strengthen the argument that the increase in sedimentary rock quantity seen across the Proterozoic-Phanerozoic boundary (Fig. 1 of the main text) is globally observed, rather than a biased product of regional geology.

Finally, we used the Australian Stratigraphic Units Database (Geoscienc Australia, 2015) to estimate rock quantity in a region not covered by Macrostrat. Each stratigraphic name in the Australian database has an age estimate and description of dominant lithologies. A time series of the age distribution of these names (10,567 in total) is shown in Fig. S3a, along with a comparative time series for stratigraphic names attached to sedimentary/metasedimentary units in Macrostrat (6,733 in total). Although there are important differences, notably in the Mesozoic and Cenozoic where there are fewer Australian stratigraphic names as compared to Macrostrat, the time series are correlated (partial correlation on first-differences with changes in interval duration held constant: $\rho = 0.54$, P = 1.5e-9; r = 0.68, P = 8.8e-16). Importantly, the two datasets share a marked increase across the end-Proterozoic.

The relationship between the number of stratigraphic names per unit time and sediment quantity is not clear. In the case of North America, however, we can investigate the connection because both stratigraphic name counts and volume totals are available. A normalized comparison suggests that number of names used to describe sediments and the volume of sediments strongly covary (Fig. S3b; partial correlation on first-differences: $\rho = 0.86$, P =2.3e-32; r = 0.91, P = 6.7e-42). The age distribution of mapped sedimentary

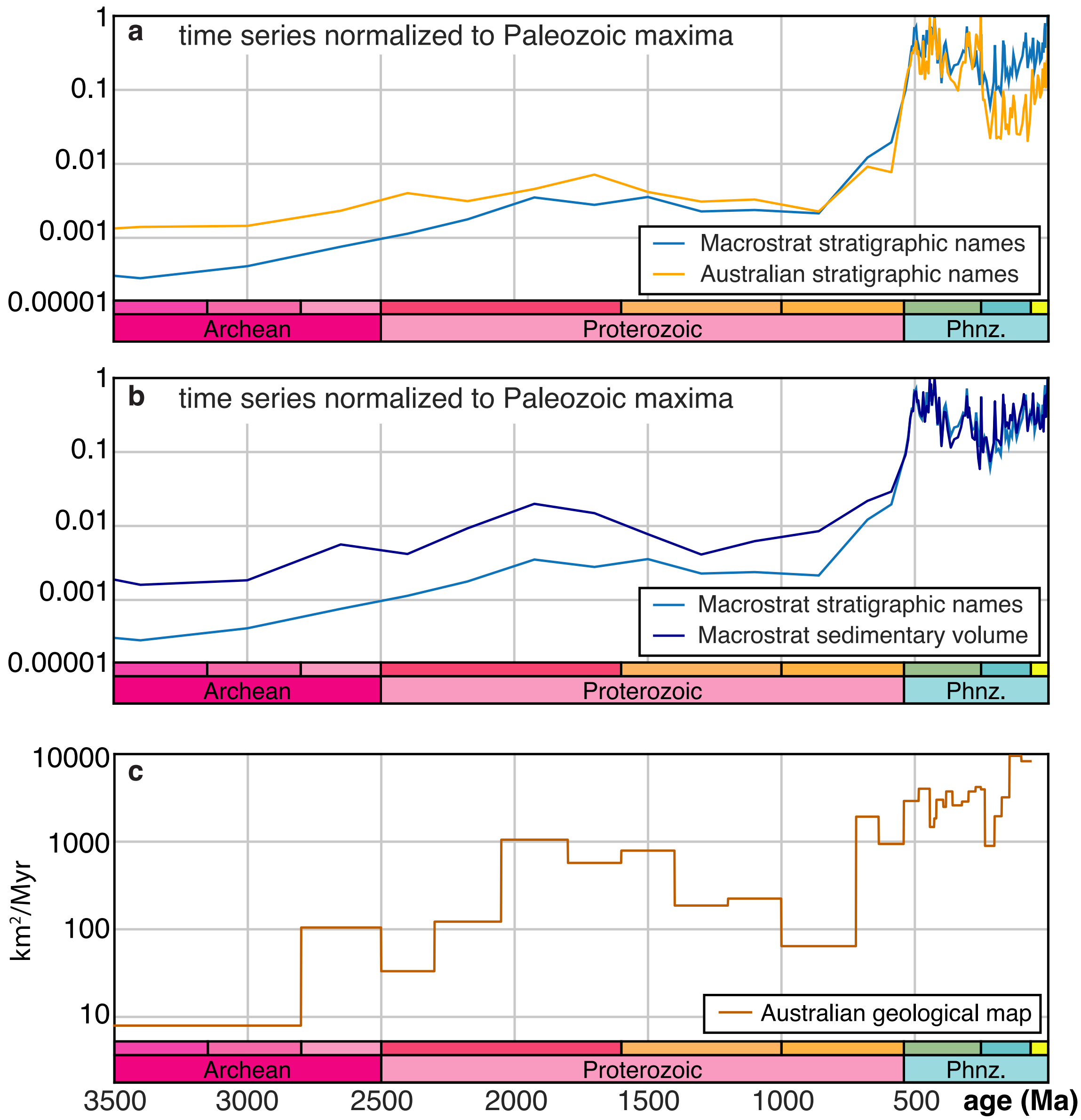

Figure S3: **Age distribution of Australian stratigraphic names.** **(a)** Time series of Australian stratigraphic names (Geoscienc Australia, 2015) and stratigraphic names associated with sedimentary/metasedimentary units in Macrostrat are shown. In **(b)**, the light blue curve is the same as in **(a)**; the dark blue curve is the sedimentary volume curve for North American Macrostrat. **(c)** The area flux of mapped sedimentary rocks, defined as (areal extent of rock body) / (duration estimate of rock body), in Australia (Raymond et al., 2012) is shown.

rocks in Australia (Raymond et al., 2012), excluding ‘regolith’, also shows a step increase in sedimentary rock area across the end-Proterozoic (Fig. S3c). This further suggests that the secular patterns in Australian stratigraphic names have a physical basis in rock abundance and that, at the broadest scale, North America and Australia share some components of temporal variability in sediment quantity with age. Ronov (Ronov et al., 1980) similarly concluded that major changes in continental sedimentation are expressed globally.

S2 Calibrating organic carbon burial

To convert sediment volume flux (e.g., Fig. 3a in the main text) to an organic carbon burial model, we used Macrostrat's lithological descriptions. In North America, 49,803 lithologies characterize 21,574 units that have a sedimentary or metasedimentary component. These lithologic descriptions are included in the unit data in Dataset S1 (under the column ‘lith’ in the output result). Although 84 unique sedimentary descriptors are used by Macrostrat, for the purposes of total organic carbon (TOC) content, we can group these lithologies into more general groups: ‘coarse-grained siliciclastics’ (dominated by sandstone and quartzite), carbonates, ‘fine-grained siliciclastics’ (dominated by shale, siltstone and slate), and ‘organic’ lithologies (dominated by coal and lignite). Together, these lithology groups account for 89% of all lithological descriptions. When one includes ‘very coarse siliciclastics’ such as conglomerates and breccias, whose TOC values are assumed to be 0, a total of 95% of all lithological descriptions currently used for North American Macrostrat are captured.

All of these lithologies have different average propensities for burying organic carbon. This statement can be demonstrated through a compilation of 5,466 TOC measurements on units from North American Macrostrat from the USGS National Geochemical

Database (USGS, 2008). Every measurement in the USGS database is paired with latitude/longitude coordinates and a stratigraphic name. Using this information, a given USGS measurement can be placed within a Macrostrat column (Fig. S1), and matching algorithms used to pair the measurement with a unit from that column. If no match is found, the search is expanded to immediately adjacent columns.

Most matches were straightforward (i.e. sample ‘Morrison Fm.’ was matched to unit named ‘Morrison Formation’), but stratigraphic nomenclatural hierarchy was also used when no direct matches were made. For example, a TOC measurement from a sample identified as belonging to the ‘Brushy Basin Member’ and collocated in a Macrostrat column where only the ‘Morrison Formation’ name is assigned to a rock unit (i.e., the members are not subdivided) would be properly linked to the unit.

A TOC dataset of this size (blue bars in Fig. S4) is large compared to studies of single stratigraphic sections or formations, but it is sparse compared to the 21,574 units that comprise the sedimentary component of the North American Macrostrat database. Thus, we utilize the associations of measurements to informal lithological characterizations, which constitute the subplots in Fig. S4. How these observed distributions should be used to define TOC loadings of Macrostrat units is not straightforward, as the scales of description are very different. All TOC data are point measurements taken from a specific position within a rock body. A Macrostrat unit, by contrast, can consist of 100’s of meters of rock thickness deposited over 1000’s of square kilometers.

Thus, rather than choosing a single TOC value for each lithological category, we define distributions for possible TOC values. For each lithology, possible values are drawn from uniform distributions, defined as $\pm 50\%$ of values given in Dataset S1. As an example, an interval of shale is assigned an equiprobable TOC value ranging between 0.95 to 2.85%. To further constrain the TOC estimates, we used 15,156 attributes that describe a subset

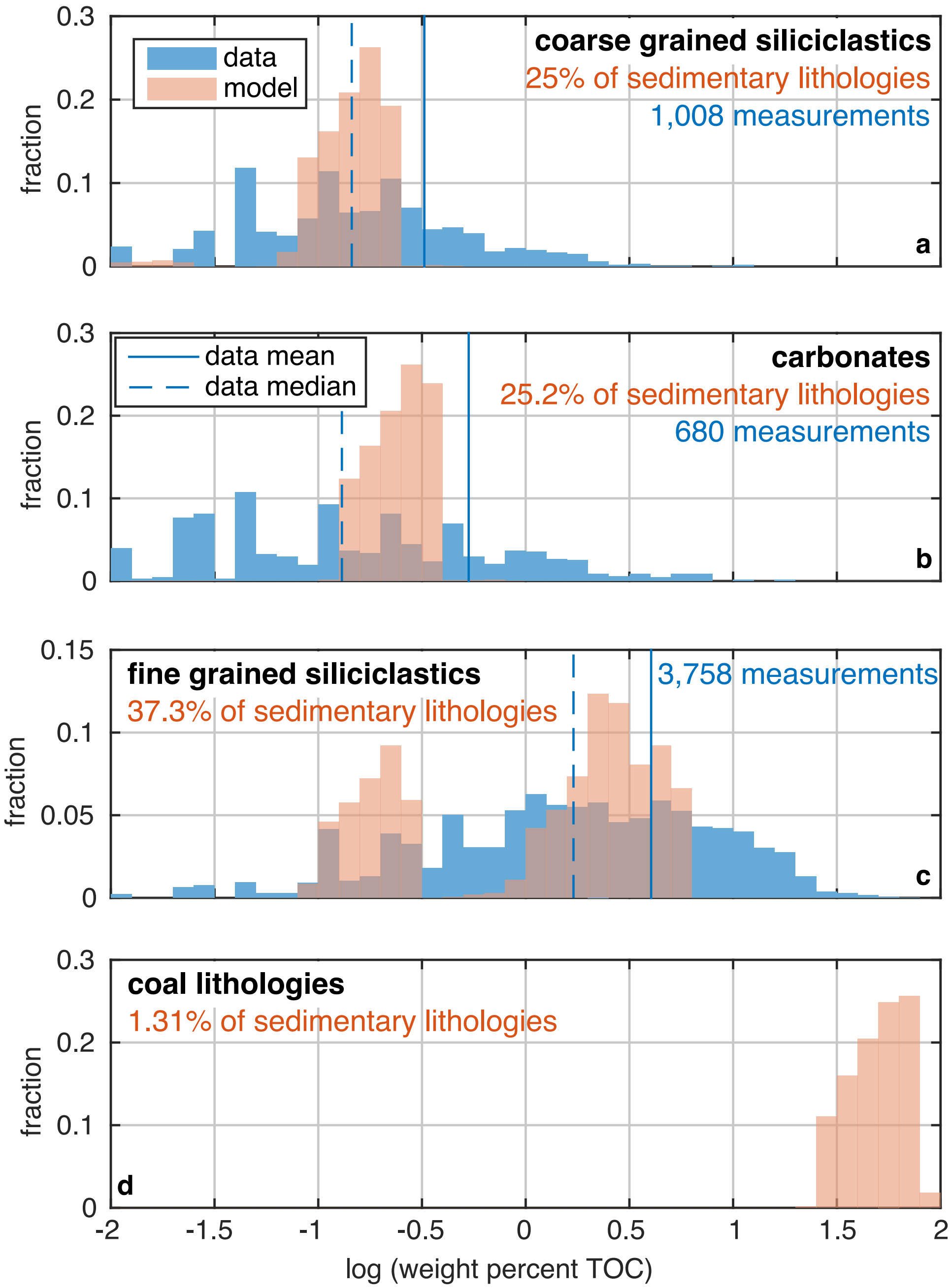

Figure S4: **Organic Carbon Model.** Distributions of modeled total organic carbon values are shown in comparison to USGS geochemical database measurements (USGS, 2008) from the same general lithologies.

of lithologies in Macrostrat, some of which are relevant to inferring its potential organic carbon load (e.g. ‘black,’ ‘red,’ ‘carbonaceous’). Although qualitative, these attributes are useful for predicting material rock properties; for example, it is expected that units with ‘black shales’ should, on average, have more organic carbon than units with ‘red shales’, even after accounting for the diagenetic and descriptive vagaries that affect the actual meaning of color-based descriptors. The initial value assigned to a lithology is, therefore, modified by the presence of relevant lithology attributes, using scale factors outlined in Dataset S1.

With a TOC value assigned to each of the 49,803 lithologies that constitute Macrostrat’s sedimentary units, the thickness, areal extent, density (also defined in Dataset S1) and the fractional abundance for each lithology per unit (a number between 0 and 1) are used to predict a molar abundance of organic carbon for a given Macrostrat unit. We take a Monte Carlo approach to help characterize the inherent uncertainty in this method; this process is repeated 1000 times, resulting in a 1000 predictions for the bulk average TOC value of every Macrostrat unit and 1000 models for organic carbon burial throughout Earth history. The red bars in Fig. S4 represent one trial, and show the predicted distributions for the different lithologic categories. The emergence of a low TOC mode for ‘fine-grained siliciclastics’ results from the presence of ‘red’ modifiers (Fig. S4c). This mode is poorly represented in the empirical data, although this observation is not surprising. Given that many TOC measurements are used for economic exploration, with red shales rarely sampled, we believe that organic-rich intervals are selectively targeted for analysis, thereby ‘biasing’ the resulting TOC distributions towards higher values. Thus, the empirical data is best viewed as point measurements of ‘black, ‘dark’ or ‘grey’ fine siliciclastics, which agree well with the high TOC mode of our model (Fig. S4c).

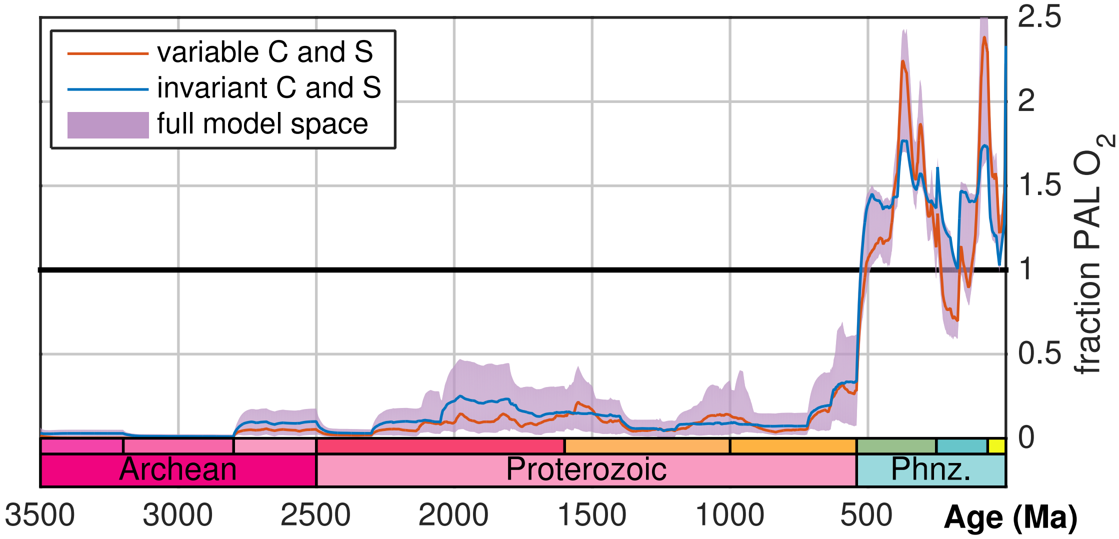

Figure S5: **Modeling atmospheric oxygen with pyrite burial.** In this iteration, the numerical model considers burial of both sedimentary organic matter and pyrite to be O_2 sources.

S3 Consideration of pyrite burial

A similar workflow for the TOC model can be used to build a model for pyrite burial, albeit with less data for comparison (the sulfur content of coal lithologies is assumed to be zero, Berner, 1984). The resulting lithology models predict a median C/S molar ratio of buried sediment to be 0.19, similar to measurements of ∼0.13 for marine sedimentary rock (Raiswell and Berner, 1986). Previous empirical pO_2 models for the Phanerozoic have included pyrite burial as a source of atmospheric oxygen (Berner and Canfield, 1989). Including it in our model would alter Equation 1 of the main text to become:

$$\frac{dM}{dt} = F_{org} + (15/8)F_S - k_1 M - k_2 B_{org}\sqrt{M} \quad ,$$

where F_S is the only new term and represents the net burial of sulfur (in moles per unit time) as sedimentary pyrite.

This parameterization results in the pO_2 forward model shown in Fig. S5. This variant shares many similarities with the carbon-only model presented in Fig. 6 of the main text. The most important similarity is the development of three relatively stable plateaus in the Archean, Proterozoic, and Phanerozoic. The main difference between the two models is that oxygen levels in the Phanerozoic are higher when pyrite burial is included than in the organic carbon-only model.

If the C and S lithology models represent a fuller accounting of the reducing power of sediment, then the results in Fig. S5 require additional sinks to bring Phanerozoic pO_2 levels closer to ~ 1 PAL. This result is sensible, as pyrite burial is an indirect source of oxygen to the surface environment. Pyrite formation requires the reduction of sulfate, which is a product of oxidative weathering of pyrite. In other words, free O_2, produced by burial of photosynthetic organic carbon, is consumed to create sulfate, and some of this bound O_2 is released subsequently as a result of microbial sulfate reduction. Thus, inclusion of pyrite as a source of atmospheric oxygen across Earth history necessitates explicit consideration of the sulfur cycle, such as the growth of the marine sulfate reservoir. For the Phanerozoic, recent work has suggested that 70 to 90% of outgoing sulfur is buried as pyrite, with inputs dominated by oxidative weathering of pyrite (Halevy et al., 2012). If correct, the net effect on atmospheric oxygen would be near zero over the residence time of sulfur, and would highlight the sulfur cycle's role as a modulator against swings in atmospheric oxygen rather than a net source or sink on long timescales.

S4 pO_2 model formulation

The source term in Equation 1 of the main text, F_{org}, is defined empirically using the flux models presented in Fig. 4 of the main text. The reaction constant for iron oxidation is defined as $k_1 = 0.0457$ Myr^{-1}, using the modern estimated consumption of O_2 during seafloor weathering of basalt (1.7×10^{18} moles O_2 Myr^{-1}, Lécuyer and Ricard, 1999).

Parameterizing oxidative weathering on land is less straightforward. In this contribution, we model oxidative weathering as having a linear dependency on the size of the sedimentary organic carbon reservoir and a weak dependency upon pO_2 (Lasaga and Ohmoto, 2002). We define k_2 using the assumption that the modern O_2 cycle is at steady state. Thus,

$$k_2 = \frac{F_{org} - F_{Fe}}{B_{org}\sqrt{M}} \quad , \tag{1}$$

where F_{Fe} is the modern flux of O_2 via iron oxidation (1.7×10^{18} moles O_2 Myr^{-1}), B_{org} is the modern size of the sedimentary organic carbon reservoir (1.25×10^{21} moles of carbon, Berner and Canfield, 1989), and M is the modern level of O_2 in the surface environment (3.8×10^{19} moles O_2). The value of F_{org} needed for defining k_2 is also difficult to determine; here, we define it as the Cenozoic average flux (excluding the Pleistocene) predicted by the organic carbon burial model presented in Fig. 4c of the main text (2.3×10^{18} moles Myr^{-1}). Thus, $k_2 = 7.286 \times 10^{-14}$ Myr^{-1} $\text{moles}^{-1/2}$. Under this formulation, oxidative weathering on land accounts for 25% of the total oxygen sink in the modern environment. Although parametrized as dependent upon the growing accumulation of sedimentary organic carbon, this O_2 consumption term implicitly includes oxidation of other reduced sedimentary phases, such as pyrite, whose accumulation in the sedimentary shell covaries with that of organic carbon deposition (Berner and Canfield, 1989).

S5 Nature of the sedimentary record

Modeling O_2 production on geological timescales using records of rock abundance through time requires that such records are relevant to inferring ancient continental sediment accumulation rates. In other words, changes in net sediment accumulation, rather than erosion and rock cycling, must control the temporal patterns in time series such as Fig. 1

of the main text. Prima facie evidence for the hypothesis that erosion is not likely to be a dominant signal is the lack of any significant long-term trend, particularly exponential decrease in quantity with increasing age, within the Phanerozoic and within the Proterozoic Eons. Ronov made the same inference when noting any lack of exponential decline in sedimentary rock quantity with increasing age in his Phanerozoic global compilation (Ronov et al., 1980).

For the Phanerozoic portion of Macrostrat, and similar global compilations (Ronov et al., 1980), the dominant signal controlling variation in sediment quantity is tectonic in origin (Meyers and Peters, 2011; Ronov et al., 1980); 76% of the variance of sedimentary coverage in North America has been attributed to the long-recognized supercontinent breakup-coalescence cycle (the 'M-curve'). A further 19% of the variance is attributed to an approximately 56-Myr oscillatory component that corresponds closely to the formation of 'tectonostratigraphic units' (Sloss, 1963), driven potentially by tectonic events on North America's margins. Similar rigorous time-series analysis has yet to be applied to the Precambrian portion of Macrostrat (Fig. 1), but the emergence of modes in the Proterozoic that are spaced by $\sim$400 Myr is suggestive that a comparable supercontinent coalescence and breakup signal is dominant in the Precambrian sedimentary record. Thus, we believe that within the Phanerozoic and within the Proterozoic, the first-order and dominant control on patterns of sedimentation is tectonic in origin (Meyers and Peters, 2011).

Nevertheless, these tectonic forcers cannot account for the dramatic change that is observed across the Precambrian-Cambrian boundary. To explain this signal, there are only two possibilities: 1) there is a step-change in the capacity of the continental crust to sequester sediments on long timescales, as is argued in the main text, or 2) erosion of a huge quantity of sediment occurred during the formation of the Great Unconformity (Peters and Gaines, 2012). The latter hypothesis is a viable alternative to the model focused on in the main text, and here we explore its attendant predictions and implications.

Figures 4 and 6 of the main text summarize a model that converts rock volumes to organic carbon burial fluxes (Fig. 4) in order to make atmospheric pO_2 predictions (Fig. 6). This model can be varied by assuming that Precambrian continental sediment fluxes were in fact comparable to Phanerozoic fluxes and that this sediment has gone missing. A hypothetical true history of continental sediment storage flux under this scenario can be constructed by sampling the observed Phanerozoic sediment fluxes for the duration of the Precambrian (dark green line in Fig. S6a). According to all estimates of surviving global sediment volumes in the Archean and Proterozoic (shaded red space in Fig. 3a of the main text), most of this Precambrian sediment must have been subsequently removed (shaded green space in Fig. S6a).

If the now-eroded volumes of Precambrian sediment were lithologically similar to existing sediments, then a potential TOC history for it can be constructed, as described above. The sediment flux time series and this 'standard' TOC history (Fig. S6b) can be used to calculate Precambrian organic carbon fluxes into continental sedimentary reservoirs. From Equation 1, the predicted pO_2 history is calculated (Fig. S6c). In this scenario, the predicted Proterozoic levels of oxygen repeatedly reach Phanerozoic-like values, which is contrary to expectations from proxy records (Sperling et al., 2015; Sahoo et al., 2012; Scott et al., 2008; Farquhar et al., 2000; Lyons et al., 2014).

Maintaining low ($\leq$10% PAL, Lyons et al., 2014) atmospheric O_2 levels while at the same time maintaining a Phanerozoic-like burial flux demands that its TOC content be comparable to the very low values shown in Fig. S6e, yielding a pO_2 history shown in Fig. S6f. This requirement can be compared directly to the empirical record. As summarized by Fig. 5 and discussion in the main text, there is little difference between Precambrian

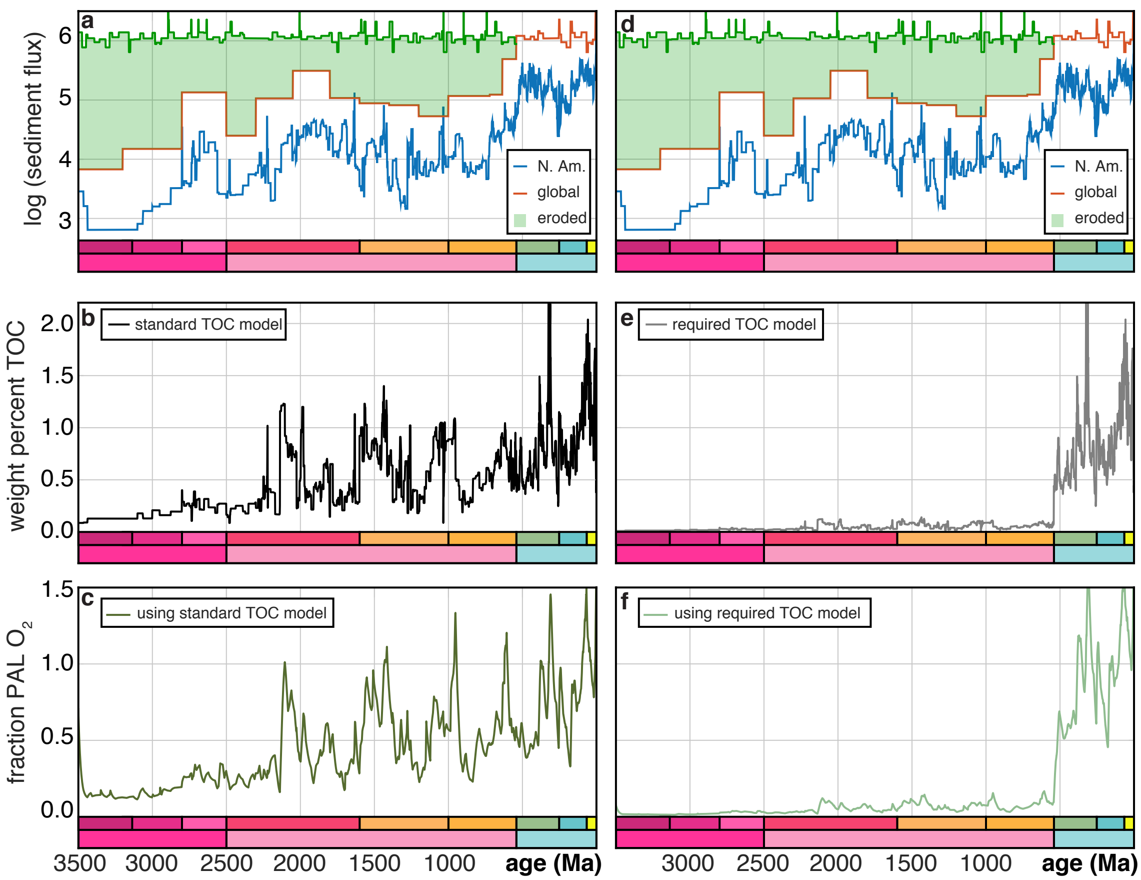

Figure S6: **Modeling experiments assuming an erosion-dominated sedimentary record and no time-variant rates of continental sedimentation. (a)** This pO_2 model experiment presupposes the existence of Phanerozoic-level sediment fluxes in continental settings (dark green curve), the majority of which has subsequently been eroded (shaded green area). **(b)** Using Macrostrat's lithological descriptions (SI Text), the TOC content of bulk sediment in North America is predicted. **(c)** Use of this 'standard TOC model' to model pO_2 according to Equation 1 of the main text results in the depicted history of atmospheric oxygen. **(d–f)** This model experiment assumes the same history of sedimentation on the continents **(d)**, but a required TOC time series is defined **(e)** to yield a pO_2 history **(f)** in alignment with proxy expectations (Lyons et al., 2014).

and Phanerozoic shale TOC content, at least among shales for which measurements have been made. Furthermore, the lithology model (above) used to produce the TOC history depicted in Fig. S6b produces formation-level TOC values for Precambrian shales (black bars in Fig. S7) that overlap with distributions of both Phanerozoic (light red line in Fig.

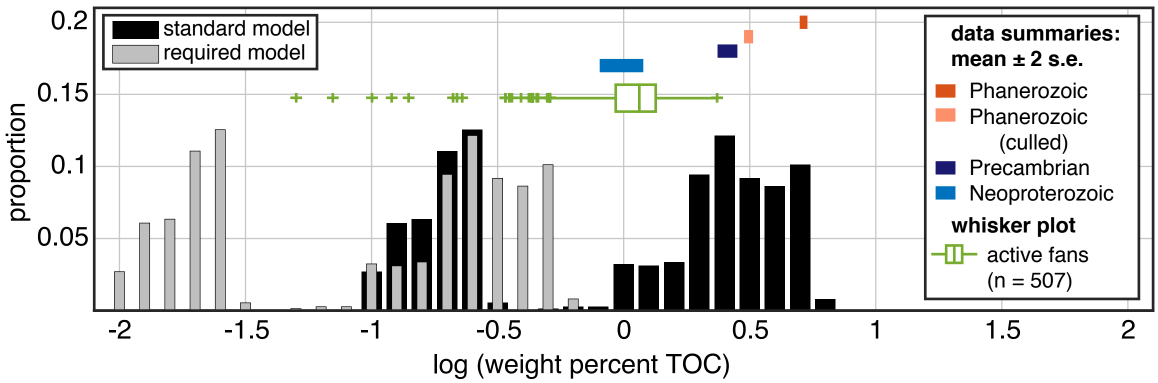

Figure S7: **Comparing TOC models to empirical data summaries.** The modeled, formation scale TOC values for Precambrian shales used to generate the pO_2 history shown in Fig. S6c are displayed as black bars ('standard model'). Also shown are the TOC model requirements in order to yield the results in Fig. S6f (grey bars, 'required model'). In each model distribution, the low TOC mode emerges from the presence of 'red' modifiers (see Methods). Summaries of shale TOC data (mean $\pm$ 2 standard errors) from Fig. 5 of the main text are shown as horizontal bars. TOC data from active Amazon (Flood et al., 1995), Mississippi (Kennicutt et al., 1986) and California margin (Yamamoto et al., 2000) submarine fans are shown also as a box and whisker plot, with individual outliers as crosses.

S7) and Precambrian shales (dark blue line in Fig. S7). Note that the low TOC mode emerges from the presence of 'red' modifiers on shale lithologies (see section S2).

By contrast, TOC values of Precambrian shales required under the constant flux scenario to meet prox pO_2 constraints are shown as the light grey bars in Fig. S7. Even average Neoproterozoic shales (light blue bar in Fig. S7), which are comparatively lean in comparison to the Paleoproterozoic and Mesoproterozoic, do not overlap with the mean TOC content required to bring the erosion-dominant model in-line with proxy records. Mean values from the Neoproterozoic in fact overlap with modern submarine fan sediments from the Amazon (Flood et al., 1995), Mississippi (Kennicutt et al., 1986) and California margin (Yamamoto et al., 2000) (box and whisker plot in Fig. S7).

Together, these results suggest that if the Proterozoic continents actually stored sediment volumes comparable to those of the Phanerozoic, and if proxy pO_2 records are generally correct, then the hypothesized and now-missing Precambrian sediment must have been very different in mean composition than surviving Proterozoic (and Neoproterozoic) sediment (Fig. S7), or that oxygen sinks were far higher in the Proterozoic. While the latter is possible, it lacks independent evidence (Derry, 2015; Keller and Schoene, 2012). Invoking a missing mass of sediment that has a distribution of TOC that is unlike any of the surviving sedimentary rock record is problematic. This suggests that Precambrian continental sediment accumulation truly was lower than Phanerozoic accumulation. This conclusion is strengthened in light of the already-strong similarities that exist between the sedimentary rock record and major biogeochemical transitions (Fig. 1), which must be disregarded as coincidental under an erosion-dominant model.

S6 Importance of deep sea burial

In the modern, 90% of organic carbon burial occurs on continental margins, with 45% occurring in coastal regions and the remaining 45% occurring in deltaic systems (Hedges and Keil, 1995). The Macrostrat data used here describes the lithostratigraphic structure of the upper continental crust of North America (Fig. S1). Thus, Macrostrat may not be ideally designed to capture and record sedimentation on margins, especially the submarine fan systems which form far offshore in deep water. The concern is valid, but accentuated by the modern state – i.e., a global low stand where continental flooding is minimal and the mean strand line is at, or near, the extent of continental crustal blocks. In Earth's past, when continental flooding was more extensive, Macrostrat (and similar, continent-focused geological syntheses, Ronov et al., 1980) does capture a substantial component of the sedimentary deposit types now forming on modern margins (see below).

A comparison of submarine fan systems that are currently active on the global continental margins (Bouma et al., 1985) and the North American sediment volumes derived from Macrostrat illustrate this point. The oldest fan sediments in the global deep sea fan data (Bouma et al., 1985) are Eocene in age, and their total volume is 12.5 million km^3 (integration of light green curve in Fig. S8a). Modern global submarine fans contain less sediment volume (82%) than the Eocene-to-modern sediments in Macrostrat's North American data (blue curve in Fig. S8a), and comprise only approximately 16% of Ronov's global sediment volume estimates across the same time span. It is also notable that these sediments are not enriched in organic carbon compared to ancient shale deposits found in continental settings (Fig. S7, Flood et al., 1995; Kennicutt et al., 1986; Yamamoto et al., 2000).

Importantly, owing to minimal continental flooding at present, the majority of modern fan volume (86%) rests on ocean crust, meaning that it will be subject to recycling and destruction on the timescale of seafloor subduction (red dashed curve in Fig. S8a, Rowley, 2002). This type of cycling and destruction is clearly observed for abyssal sediments in Macrostrat (dark green curve in Fig. S8a; deep sea core locations are green squares on the world map). Given the location of deep sea fans along continental margins, it is reasonable to hypothesize that they recycle even faster than average abyssal ocean sediments, a possibility supported by the steeper slope for the active fan time series as compared to deep sea sediments (Fig. S8a). It is also possible that the present extent and volume of submarine fans is unusually large, relative to the average state of the Phanerozoic, because of the overall decline in the extent of continental fooding from the Cretaceous high-stand to the present (Ronov, 1994). Within Macrostrat, the number of submarine fans decreases over this same interval (Fig. S8b), a decline that potentially reflects this shift in the locus of fans further out towards continental margins.

It is important to note that during times of higher continental flooding, Macrostrat can

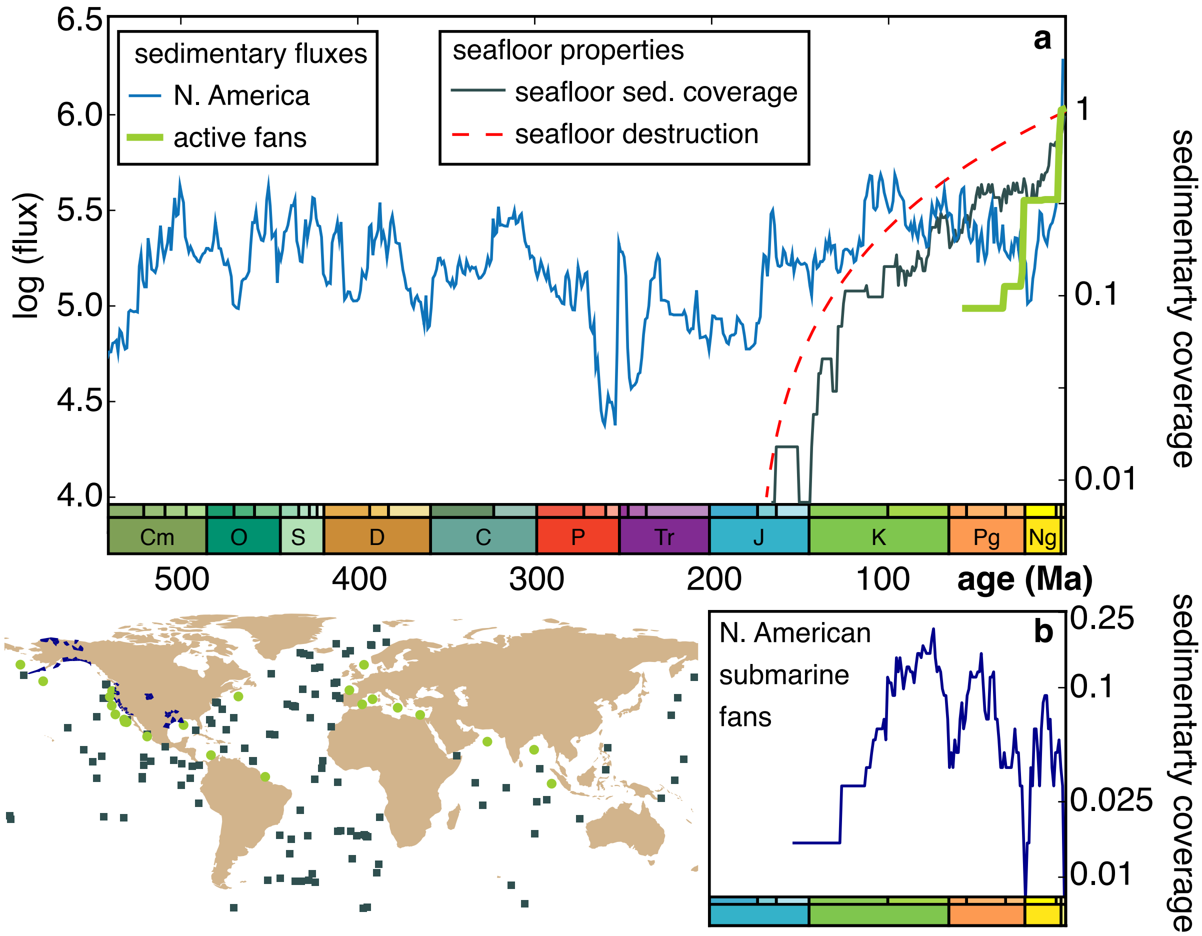

Figure S8: Time series of North American sediment flux, as estimated by Macrostrat (Fig. S1), and modern active fans (Bouma et al., 1985) are displayed for the Phanerozoic. Units are km^3 per million years. The right y–axis shows the sedimentary coverage of ocean floor as measured by the deep sea portion of Macrostrat (dark green curve), as well as a normalized model for seafloor subduction (red dashed curve, Rowley, 2002). **(b)** For comparison, the abundance of Mesozoic and Cenozoic seafloor fans in Macrostrat is displayed. Global map shows the locations of these ancient fans (dark blue polygons), modern fans (light green circles from Bouma et al., 1985) and deep sea sediment cores contained within the Macrostrat database (dark green squares). Data to produce the sedimentary coverage of ocean floor time series are available at `https://macrostrat.org/api/v2/units?project_id=4&lith_class=sedimentary&lith_type=metasedimentary&format=csv`

capture submarine fan systems, which then persist in the long-term sedimentary record by virtue of being located on continental instead of oceanic crust. As an example, all of the ancient North American fans in the Bouma et al. (1985) compilation are represented in Macrostrat (Fig. S8b). This observation is important because fans located on the region captured by Macrostrat are part of the long-term sediment reservoir whereas fans that are not captured by Macrostrat, like those of today, can have their reducing power returned to the surface environment on the timescales of seafloor destruction and therefore do not constitute long-term net sediment accumulation (Fig. S8a). The contention that the accumulation of crustal organic carbon, and resulting net oxidation of the surface environment, depends critically (if not entirely) on continental storage of sediment is not new (Hayes and Waldbauer, 2006; Berner and Canfield, 1989; Lee et al., 2016). Our results, however, are the first to demonstrate empirical covariation between the long-term history of continental sediment accumulaiton and estimates for atmospheric pO_2 (Fig. 1 of the main text).

S7 A possible Paleoproterozoic Great Unconformity?

A model of constant, Phanerozoic-like continental sedimentary fluxes throughout Earth history is unlikely (section S5 and Fig. S6). However, alternative models, which do depend upon a subordinate signature of some erosion, can be explored. Specifically, we hypothesize here that the formation of a 'Great Unconformity' accumulated a Phanerozoic-like mass of sediment in the Paleoproterozoic, but that this mass has been lost to erosion and the formation of the most recent iteration of the Great Unconformity process.

We base this hypothesis on Macrostrat's time series of sediment area with time (Fig. S9a), which shows a Proterozoic maximum at $\sim$1800 Ma. It is possible that this feature reflects an erosional remnant of a Phanerozoic-like volume of sediment that formed during the first 'Great Unconformity-like' transition in the ability of the continents to serve as long-term sediment storage reservoirs. In this scenario, erosional loss of the Paleoprotero-

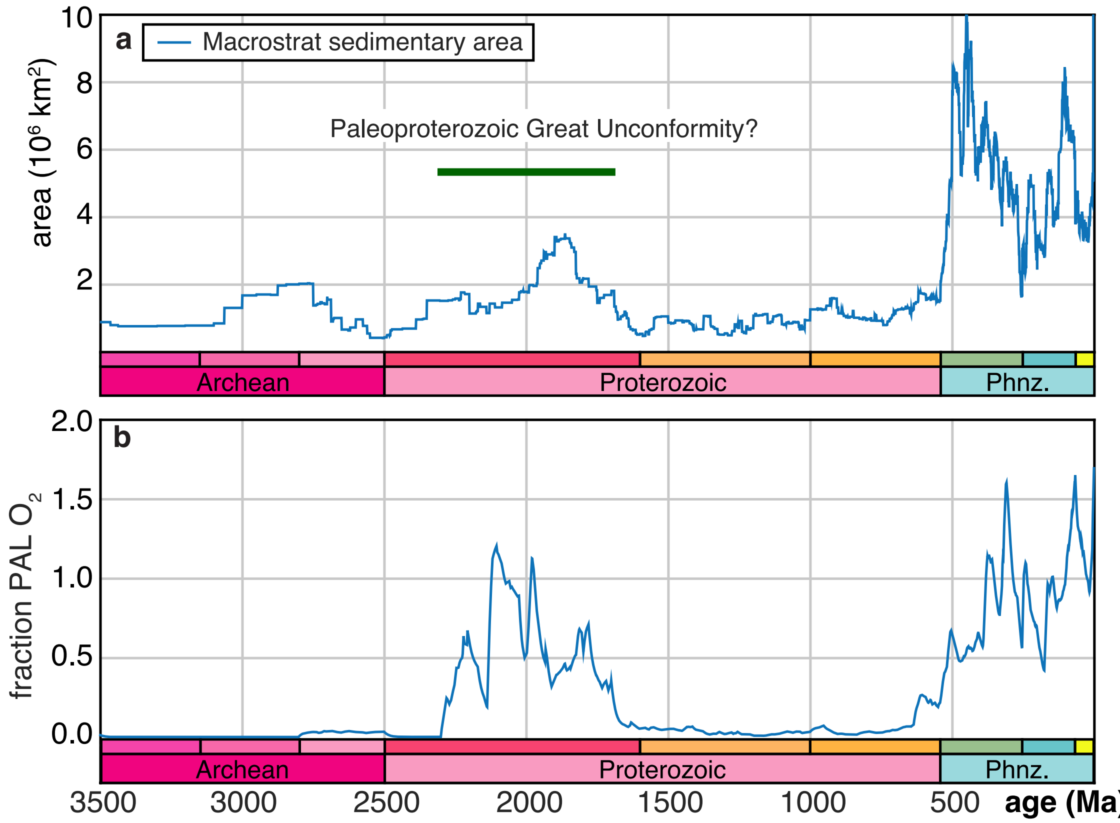

Figure S9: **Evidence for multiple Great Unconformities? (a)** Given evidence for a local maximum in sedimentary area in North American Macrostrat at ~2000–1800 Ma, we consider a model variant wherein continental sediment fluxes were high in the early Paleoproterozoic. **(b)** According to Equation 1 of the main text, this pO_2 history results if the TOC model shown in Fig. S6c is used.

zoic sediment then occurred during the following billion years, perhaps accelerated during the formation of the Precambrian-Cambrian bounding Great Unconformity. Although this hypothesis is very speculative, if it is assumed that there was in fact a 'Paleoproto-erozoic Great Unconformity' that established a (now destroyed) Phanerozoic-scale volume of sediment, and if it is further assumed that this volume of sediment was compositionally similar to the surviving Proterozoic sediments, then this scenario predicts a pronounced, but also transient, rise in atmospheric oxygen (Fig. S9b).

The data are insufficient at this time to advocate strongly for this model, particularly given the explanatory power of the simpler model that treats the sedimentary rock record as a consistent proxy for net continental sediment accumulation (Fig. 1). However, this model is consistent with some emerging ideas about the history of atmospheric oxygen, which includes the hypothesis that O_2 rose to modern levels following the Great Oxidation event at ~ 2.2 Ga, and subsequently fell to below 10% PAL in the early Proterozoic (Lyons et al., 2014).

This hypothesis does also raise the provocative possibility that the continental burial flux and attendant long-term storage of organic carbon necessary to maintain an oxygen-rich atmosphere is not sustained indefinitely as a planetary process. If the current episode of Phanerozoic continental sediment storage does come to end, and if the locus of sedimentation continues to be focused along continental margins that are much more readily recycled, then the future may see a crash in atmospheric oxygen, similar to that which occurred at the end-Permian (Fig. 6). If continental sediment storage does not resume, as it did during the Mesozoic (Fig. 1), then that $p\mathrm{O}_2$ crash may continue, eventually reaching levels not seen since the Proterozoic.

References

Berner, R. A., 1984, Sedimentary pyrite formation: an update: Geochimica et cosmochimica Acta, vol. 48, pp. 605–615.

Berner, R. A. and Canfield, D. E., 1989, A new model for atmospheric oxygen over Phanerozoic time: Am. J. Sci, vol. 289, pp. 333–361.

Bouma, A. H., Normark, W. R., and Barnes, N. E., eds., 1985, Submarine fans and related turbidite systems: Springer-Verlag.

Derry, L. A., 2015, Causes and consequences of mid-Proterozoic anoxia: Geophysical Research Letters, vol. 42, pp. 8538–8546.

Farquhar, J., Bao, H., and Thiemens, M., 2000, Atmospheric influence of Earth's earliest sulfur cycle: Science, vol. 289, pp. 756–758.

Flood, R., Piper, D., Klaus, A., and et al., eds., 1995, Proceedings of the Ocean Drilling Program, Initial Reports: Site 931, vol. 155: Ocean Drilling Program.

Gesocience Australia, 2015, Australian stratigraphic units database: Tech. rep.

Garrity, C. and Soller, D., 2009, Database of the Geologic Map of North America; adapted from the map by J.C. Reed, Jr. and others (2005): Data Series 424, U.S. Geological Survey.

GSC, 1995, Generalized geological map of the world and linked databases: Open File Report 2915d, Geological Survey of Canada.

Halevy, I., Peters, S. E., and Fischer, W. W., 2012, Sulfate burial constraints on the Phanerozoic sulfur cycle: Science, vol. 337, pp. 331–334.

Hayes, J. M. and Waldbauer, J. R., 2006, The carbon cycle and associated redox processes through time: Philosophical Transactions of the Royal Society B: Biological Sciences, vol. 361, pp. 931–950.

Hedges, J. I. and Keil, R. G., 1995, Sedimentary organic matter preservation: An assessment and speculative synthesis: Marine Chemistry, vol. 49, pp. 81–115.

Keller, C. B. and Schoene, B., 2012, Statistical geochemistry reveals disruption in secular lithospheric evolution about 2.5 Gyr ago: Nature, vol. 485, pp. 490–493.

Kennicutt, M., Defreitas, D., Joyce, J., and Brooks, J., 1986, Nonvolatile organic matter in sediments from Sites 614 to 623, Deep Sea Drilling Project Leg 96: Tech. rep., Deep Sea Drilling Project.

Lasaga, A. C. and Ohmoto, H., 2002, The oxygen geochemical cycle: dynamics and stability: Geochimica et Cosmochimica Acta, vol. 66, pp. 361–381.

Lécuyer, C. and Ricard, Y., 1999, Long-term fluxes and budget of ferric iron: implication for the redox states of the Earth's mantle and atmosphere: Earth and Planetary Science Letters, vol. 165, pp. 197–211.

Lee, C.-T. A., Yeung, L. Y., McKenzie, N. R., Yokoyama, Y., Ozaki, K., and Lenardic, A., 2016, Two-step rise of atmospheric oxygen linked to the growth of continents: Nature Geoscience, vol. 9, pp. 417–424.

Lyons, T. W., Reinhard, C. T., and Planavsky, N. J., 2014, The rise of oxygen in Earth's early ocean and atmosphere: Nature, vol. 506, pp. 307–315.

Meyers, S. R. and Peters, S. E., 2011, A 56 million year rhythm in North American sedimentation during the Phanerozoic: Earth and Planetary Science Letters, vol. 303, pp. 174–180.

Peters, S. E. and Gaines, R. R., 2012, Formation of the 'Great Unconformity' as a trigger for the Cambrian explosion: Nature, vol. 484, pp. 363–366.

Raiswell, R. and Berner, R. A., 1986, Pyrite and organic matter in Phanerozoic normal marine shales: Geochimica et Cosmochimica Acta, vol. 50, pp. 1967–1976.

Raymond, O., Liu, S., Gallagher, R., Highet, L., and Zhang, W., 2012, Surface geology of Australia, 1:1 000 000 scale, 2012 edition [digital dataset]: Tech. rep., Geoscience Australia, Commonwealth of Australia, Canberra.

Ronov, A., Khain, V., Balukhovsky, A., and Seslavinsky, K., 1980, Quantitative analysis of Phanerozoic sedimentation: Sedimentary Geology, vol. 25, pp. 311–325.

Ronov, A. B., 1994, Phanerozoic transgressions and regressions on the continents: a quantitative approach based on areas flooded by the sea and areas of marine and continental deposition: American Journal of Science, vol. 294, pp. 777–801.

Rowley, D. B., 2002, Rate of plate creation and destruction: 180 Ma to present: Geological Society of America Bulletin, vol. 114, pp. 927–933.

Sahoo, S. K., Planavsky, N. J., Kendall, B., Wang, X., Shi, X., Scott, C., Anbar, A. D., Lyons, T. W., and Jiang, G., 2012, Ocean oxygenation in the wake of the Marinoan glaciation: Nature, vol. 489, pp. 546–549.

Scott, C., Lyons, T. W., Bekker, A., Shen, Y., Poulton, S. W., Chu, X., and Anbar, A. D., 2008, Tracing the stepwise oxygenation of the Proterozoic ocean: Nature, vol. 452, pp. 456–459.

Sloss, L., 1963, Sequences in the cratonic interior of North America: Geological Society of America Bulletin, vol. 74, pp. 93–114.

Sperling, E. A., Wolock, C. J., Morgan, A. S., Gill, B. C., Kunzmann, M., Halverson, G. P., Macdonald, F. A., Knoll, A. H., and Johnston, D. T., 2015, Statistical analysis of iron geochemical data suggests limited late Proterozoic oxygenation: Nature, vol. 523, pp. 451–454.

USGS, 2008, Geochemistry of rock samples from the national geochemical database: Tech. rep., U.S. Geological Survey.

Yamamoto, M., Yamamuro, M., and Tada, R., 2000, Late Quaternary records of organic carbon, calcium carbonate, and biomarkers from site 1016 off Point Conception, California Margin: Tech. rep., Ocean Drilling Program.